Electronic Supplementary Information

Bifunctional Au-Mn_3O_4 nanocomposites: Benign electrocatalysts towards water oxidation and oxygen reduction

Hasimur Rahaman, Koushik Barman, Sk Jasimuddin, and Sujit Kumar Ghosh*

Department of Chemistry, Assam University, Silchar-788011, India

E-mail: sujit.kumar.ghosh@aus.ac.in

ESI 1. Experimental

A schematic presentation showing the formation of Au-Mn_3O_4nanocomposites is shown in Scheme SI 1.

Scheme SI 1. Schematic presentation of the synthesis of Au-Mn_3O_4 nanoparticles

The particles formed by this method were used as electrocatalysts for water oxidation reaction.

ESI 2.Characterization of the evolution of the nanocomposites

Absorption spectroscopy. The absorption spectral features of Au, Mn_3O_4 and Au-Mn_3O_4 particles are presented in Fig. SI 1. Gold nanoparticles exhibit an absorption spectrum with maximum at 520 nm corresponding to the characteristic surface plasmon resonance of conduction electrons of the particles. The electronic absorption spectrum of manganese oxide nanoparticles shows three well-defined regions: the first portion from 250 to 425 nm, thesecond from 425 to 585 nm and the third one finishing at 700 nm. The first portion is attributed to the allowed $O^{2-} \rightarrow Mn^{2+}$ and $O^{2-} \rightarrow Mn^{3+}$ charge transfer transitions (A. Vázquez-Olmos, R. Redón, A. L. Fernández-Osorio, J. M. Saniger, *Appl. Phys. A* 2005, **81**, 1131–1134), and the last two can be reasonably related to d-d crystal field transitions, $^3E_g(G) \leftarrow {}^3T_{1g}$, $^3A_{2g}(F) \leftarrow {}^3T_{1g}$, $^3A_{2g}(G) \leftarrow {}^3T_{1g}$, $^3T_{2g}(H) \leftarrow {}^3T_{1g}$, $^3T_{1g}(H) \leftarrow {}^3T_{1g}$ and $^3E_g(H) \leftarrow {}^3T_{1g}$, on octahedral Mn^{3+} species (W. S. Kijlstra, E. K. Poels, A. Bliek, B. M. Weckhuysen, R. A. Schoonheydt *J. Phys. Chem. B* 1997, **101**, 309–316). In the spectrum of the nanocomposites,

it is seen that the portion of the absorption band due to charge transfer transition of manganese oxide and the surface plasmon band of gold vanishes indicative of strong metal-support interaction (K. S. Kim, N. Winograd, *Chem. Phys. Lett.* 1975, **30**, 91–95).

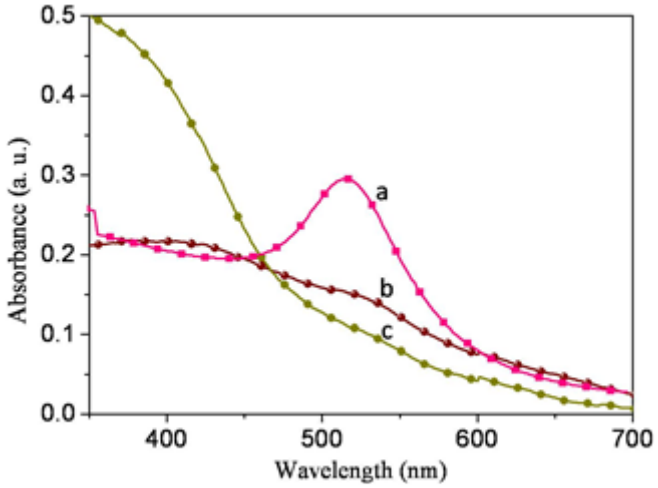

Fig. SI 1. Absorption spectra of (a) Au, (b) Mn_3O_4 and (c) Au-Mn_3O_4 nanoparticles

Fourier transform infrared spectroscopy. Fig. SI 2 represents the FTIR spectra of Mn_3O_4nanoparticles before and after addition of gold nanopartcles. The presence of Mn-O stretching vibrations at 455, 505, 588 and 634 cm^{-1} (trace a) confirms the presence of Mn_3O_4as the major phase (X. Tanga, J. Li, L. Suna, J. Hao, *Appl. Catal. B* 2010, **99**, 156–162). After the deposition of gold nanoparticles (trace b), the band at 455 cm^{-1} is shifted to 459 cm^{-1} and the bands at 505, 588 and 634 cm^{-1}almost vanishes indicating the attachment of gold with the manganese oxide nanostructures.

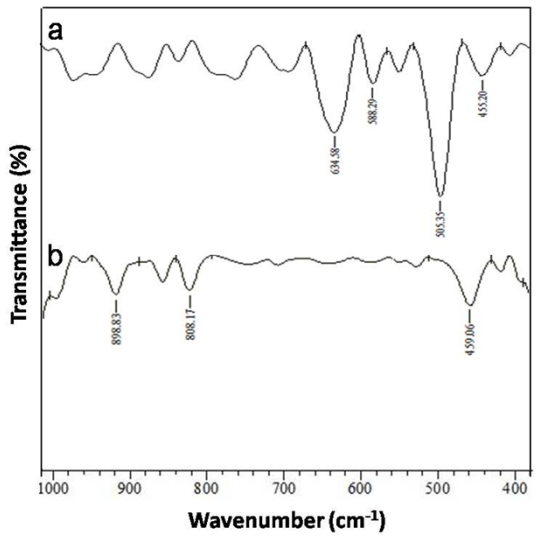

Fig. SI 2. FTIR spectra of Mn_3O_4 (a) before and (b) after addition of gold nanoparticles

X-ray diffraction pattern. X-ray diffraction pattern of Au-$Mn_3O_4$is shown in Fig. SI 3. On the basis of the position and relative intensity, all diffraction peaks could be indexed to standard fcc structured Au and tetragonal hausmannite structure of Mn_3O_4 nanoparticles with lattice parameters a = b = 5.762 Å, and c = 9.469 Åand space group $I4_{I/amd}$, which are consistent with the standard values of bulk Mn_3O_4 (JCPDS# 24-0734) (T. Ahmad, K. V. Ramanujachary, S. E. Lofland, A. K. Ganguli, *J. Mater. Chem.* 2004, **14**, 3406–3410).

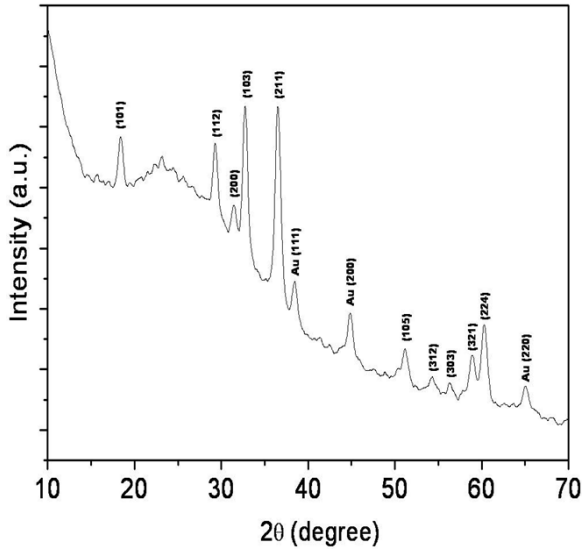

Fig. SI 3. X-ray diffraction pattern of Au-Mn_3O_4 nanocomposites

ESI 3. Modification of the gold electrodes for the study of electrocatalytic activity. To investigate the electrocatalytic activity, the gold electrode was modified as described below. At first, the gold electrode was polished with 0.05 μm alumina powder on a polishing microcloth and rinsed, methodically, with distilled water. The mechanically cleaned electrode was decontaminated electrochemically in 1.0 M H_2SO_4 solution. A reproducible cyclic voltammogram between -0.2 to +1.5 V *vs.* Ag/AgCl electrode ascertained the cleanliness of the electrode. The electrode was, then, soaked with distilled water and subsequently,dipped in 10 mM 4-aminothiophenol (4-ATP) solution for 20 h to allow the formation of self-assembled monolayer (SAM) over gold surface. After that, the 4-ATP functionalized gold electrode was washed thoroughly with distilled water and placed in 10 μM colloidal dispersion for the desired period to obtain the nanoparticles-modified electrode.The modification of the gold electrode with the nanoparticles is shown schematically in Scheme SI 2.

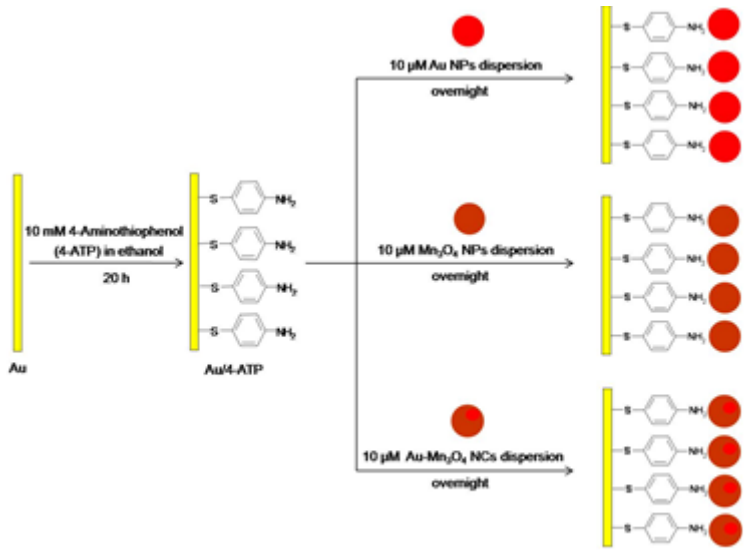

Scheme SI 2. Modification of the gold electrode with Au, Mn_3O_4 and Au-Mn_3O_4 nanoparticles

Electrochemical impedance spectroscopy of 1.0 mM $[Fe(CN)_6]^{3-/4-}$ in 0.1 M PBS at bare, 4-ATP modified and NPs or NCs-immobilized gold electrode is shown in Fig. SI 4. It is seen that the charge transfer resistance (R_{CT}) is very high when the gold electrode surface was modified with self-assembled monolayer (SAM) of 4-ATP (brown) than bare gold (black). The electronic communication between the redox species $[Fe(CN)_6]^{3-/4-}$ in solution and the underlying gold electrode becomes restricted due to formation of SAM. After the immobilization of NPs on 4-ATP/gold electrode, the R_{CT} decreased indicating that the NPs were, successfully, immobilized on the 4-ATP modified gold electrode and a good electronic communication was attained between the redox species $[Fe(CN)_6]^{3-/4-}$ in solution and the underlying Au electrode through NPs.

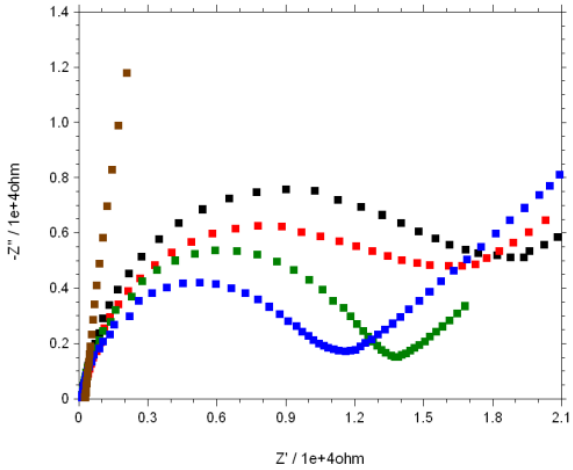

Fig. SI 4. Overlaid Nyquist plot ($-Z''$*vs.*Z') for 1.0 mM $[Fe(CN)_6]^{3-/4-}$in 0.1 M PBS (pH 7.5) at bare gold (black), 4-ATP/gold (brown), Au NPs/4-ATP/gold (red), Mn_3O_4NPs/4-ATP/gold (green) and Au-Mn_3O_4NCs/ATP/gold (blue) electrodes, where, anodic current amplitude, E_{ac} = 10 mV while the frequency varies from 0.01 - 100000 Hz.

ESI 4. Study of water oxidation reaction with different sizes of the gold nanoparticles in the composites. To study the efficacy of the electrocatalytic activity of the gold-manganese oxide nanocomposites, three different sizes of gold nanoparticles (*viz.*, 10, 16, and 25 nm by varying [Au(III)]/[citrate] ratio as 5.0, 3.5, and 2.5 respectively) prepared by Frens' citrate reduction procedure (G. Frens, *Nature* 1973, **241**, 20-22) were employed for the preparation of gold-manganese oxide nanocomposites and their electrocatalytic activity was studied towards oxygen reduction reaction. It is seen that Au(10)-Mn_3O_4 are more efficient catalysts for water oxidation reaction than Au(16)-Mn_3O_4 and Au(25)-Mn_3O_4 composites (Fig. SI 5).

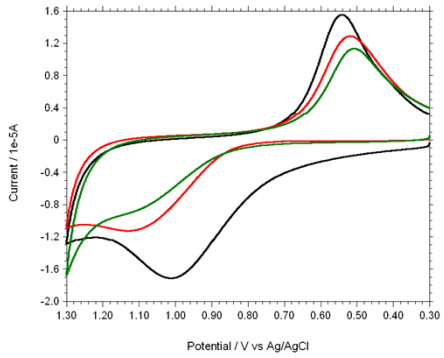

Fig. SI 5. Cyclic voltammogram for the water oxidation at Au(10)-Mn_3O_4 (black), Au(16)-Mn_3O_4 (red) and Au(25)-Mn_3O_4 (green)-modified gold electrode in 0.1 M PBS at pH~7.5.

ESI 5. Simultaneous oxygen reduction reaction during water oxidation

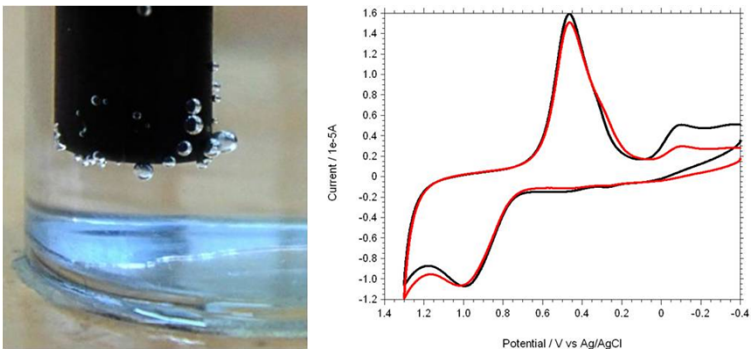

Figure SI 6.(left) Digital camera photograph showing oxygen gas evolution during water oxidation reaction; (right) cyclic voltammogram of oxygen reduction of Au-Mn_3O_4 NCs/4-ATP/gold electrodes under ambient (black) and N_2-saturated (red) PBS at pH~7.5.

ESI 6. Overpotentoial of the Au-Mn_3O_4 nanocomposites and some other electrocatalysts

Table SI 1. A comparative account of the pH condition of the experiment and overpotential of the Au-Mn_3O_4 and some other electrocatalysts

Catalyst	pH	Overpotential (mV)	Reference
IrO_x	13.0	290	Murray et al. [Ref. 12]
Nickel Film	14.0	1070	Dai et al. [Ref. 14]
$Co(III)_3Co(IV)O_4$	9.5	350-430	Britt et al. [Ref. 15]
copper–bipyridine	11.8 – 13.3	750	Mayer et al. [Ref. 17]
Au-Mn_3O_4	7.5	370	Present work